Charging and Plasma Effects under Ultrashort Pulsed Laser Ablation[1]

N.M. Bulgakova and V.P. Zhukov*

Institute of Thermophysics SB RAS, 1, Lavrentyev ave., 630090, Novosibirsk, Russia
Phone: +8(383) 330-10-95, Fax: +8(383) 330-84-80, E-mail: nbul@itp.nsc.ru
**Institute of Computational Technologies SB RAS, 6, Lavrentyev ave., 630090, Novosibirsk, Russia*

Abstract – Femtosecond laser ablation of solid targets is strongly affected by the presence of a dense ambient atmosphere due to several effects including pressure confinement, ambient plasma formation, gas-phase chemistry, and plasma-surface interaction. We study the influence of ambient plasma on the dynamics of heating of metallic targets which was recently found for femtosecond laser ablation in a gas environment. To gain a better insight into the plasma effects, a combined model has been developed, based on 2D thermal modeling of laser-induced heating of a metal target (platinum as an example) and description of dynamics of the ambient gas (argon) perturbed by a sudden heat release (laser energy absorption) in the laser focus region in front of the irradiated spot. Additionally a model of laser-induced breakdown of an ambient gas in a focal region in front of the irradiated target has been proposed. The simulation results demonstrate an intriguing picture of laser-induced ambient gas motion and shock wave formation that causes additional heating of the target and can strongly affect the ablation process. Plasma-chemical reactions on the sample surface and their effect on the laser ablation dynamics and surface modification are discussed.

1. Introduction

Femtosecond laser ablation has been demonstrated to be a powerful tool for both fundamental studies and various technologies [1]. Due to rapid energy delivery, the laser-plume interaction is avoided and heat-affected zones in the irradiated targets are strongly localized with minimal residual damage. This allows generation of well-defined microstructures with high quality and reproducibility [2]. However, for further development of the pulsed laser technologies, a detailed understanding of the dynamics and mechanisms of particle desorption and ablation from the irradiated surfaces is of crucial importance.

An important issue is the role of ambient plasma in laser material processing. Since in the majority of technological applications, material processing by fs laser pulses is carried out in an ambient environment (air, inert or reactive gases, liquid media), the question arises about ambient medium breakdown and how the ambient plasma can intervene in the process. Plasma etching of different surfaces is a widely studied phenomenon due to its extensive usage in plasma-chemical technologies [3]. Even plasma of an inert gas becomes an etching agent when its energetic ions bombard the contiguous surfaces. Plasma of highly reactive gases leads to strong corrosion of surfaces. Liquid media such as water and organics used for laser-assisted nanoparticle production [4–5] gain high reactive properties when reaching their near-critical thermodynamic states [6]. Here we make an attempt to analyze the laser breakdown process in the ambient gas under femtosecond laser ablation of metals, to follow the dynamics of the ambient gas motion induced by the laser energy coupling, and to discuss the consequences of plasma-target interaction in laser material processing.

2. Ambient plasma formation under ultrashort laser ablation: heat exchange model

A strong influence of the ambient plasma on the dynamics of heating of metallic targets was recently reported for femtosecond laser ablation in a gas environment resulting in significant enhancement in thermal energy retained in targets [7–8]. In the past, this effect was also observed for nano- and microsecond laser pulses and explained by energy transfer from plasma to the sample [9–12]. Theoretical models of energy transfer from plasma to a sample have been previously developed for long laser pulses when a laser-supported combustion waves are near the sample [9]. However, the gasdynamic motion in the ambient plasma was not considered in these models [9] and this is an important distinction of our model. Due to the extreme complexity of a general model which includes laser-induced formation of the ambient plasma and its gasdynamic motion with conduction and radiation energy transfer from the plasma, we split the problem into two ones. In this Section we describe a combined model, based on 2D thermal modeling of laser-induced heating of a metal target (platinum as an example) and description of dynamics of an ambient gas (argon) perturbed by a sudden heat release (laser energy absorption) in front of the irradiated spot [13].

[1] The work was performed under financial support by INTAS/SB RAS (Grant No. 06-1000013-8949) and RFBR (Grants Nos. 08-01-00264 and 08-08-00756).

In the gas breakdown process, seed electrons can be produced by multiphoton ionization, electrons photo-emitted from the irradiated target, and ambient gas contamination with the ablated nano- and microparticles, depending on irradiation conditions. For pulse durations $\tau \sim 100$ fs, the seed electrons can be generated only by multiphoton ionization as the avalanche development needs times of several ps [13]. Assuming that breakdown occurs in the focusing zone (in Refs. [7, 8] the irradiation spot radius R_L is ~ 100 μm and the focus length is ~ 100 – 200 μm), we can estimate the generated electron population in an ambient gas [14] as

$$\partial n_e / \partial t = A n_a I_0^k(t), \quad (1)$$

where n_a is the density of neutral atoms; $I_0(t)$ is the temporal shape of the incident laser pulse; k and A are the order and rate constants of the multiphoton ionization. In the absence of data for 800 nm laser wavelength as in Refs. [7, 8], we make estimates for longer and lower wavelengths, 1.06 μm (Nd^{3+} laser) and 694 nm (ruby laser) [14]. For Ar at 1.08 atm, we obtain that 100% single ionization is reached in the focus region already at fluence of 3 J/cm^2 for both wavelengths and, hence, for 800 nm. For He, 100% single ionization is reached only at ~ 4–5 J/cm^2 that agrees with the experimental data on the onset of enhanced target heating [7]. We also note that, immediately above the metallic surface, the front part of the laser beam reflected from the target can interfere with the incident pulse tail producing interference maxima where the probability of multiphoton ionization is enhanced by several orders of magnitude. Although the interference region is limited to a half-length of the wave packet (~ 20 μm for our case), one can expect double ionization in this narrow region at fluences ≥ 1 J/cm^2. This effect enhances absorption of radiation by the ambient gas.

Thus, the scenario of laser-induced ambient gas ionization under fs laser ablation conditions of metal targets can be considered as follows.

Substantial ionization in the immediate vicinity of the target due to self-interference of the laser beam can be reached in atmospheric-pressure argon at fluences ~ 0.3–0.4 J/cm^2.

However, the pronounced ionization effect is reached when direct multiphoton ionization develops in the focal zone above the target. The produced plasma survives up to several nanoseconds [15]. This plasma transmits its energy to the sample via the heat conduction and radiation processes.

We consider a following simplified problem. A Pt sample is irradiated with a fs laser pulse at 800 nm wavelength with fluence F_0 of 3 J/cm^2 [7, 8]. The absorbed laser energy $(1 - R)F_0\pi R_L^2$ is instantaneously distributed in the sample as $\exp(-\alpha z - r^2/R_L^2)$, where z and r are axial and radial coordinates; α and R are the absorption and reflection coefficients; $R_L = 50$ μm.

Argon near the sample (1.08 atm, 20 °C) is singly ionized in a region with a 100-μm thickness (Z_L) and radius R_L; and the ionization energy is immediately converted into the gas heat. The initial temperature is distributed as $T = T_0 + T_L \exp(-r^2/R_L^2 - z^2/Z_L^2)$, where T_0 is the initial (room) temperature and $T_L = T_{ion} + T_{add}$ with T_{ion} being equal to $(\gamma - 1)I_{\mathrm{Ar}}$ (I_{Ar} is the first ionization potential of argon expressed in Kelvin). Due to interference effect, there can be an additional effect of laser energy absorption by argon and we introduce T_{add} as $T_{add} = \varepsilon(\gamma - 1)Rk_BF_0/(n_aZ_L)$ with ε representing the absorbed fraction of the reflected light and k_B being the Boltzman constant. Heat evolution in the sample, hydrodynamics of the ambient gas and heat exchange between the target and argon are described by the following equations:

$$\frac{\partial \rho}{\partial t} + \mathrm{div}\left(\rho \vec{V}\right) = 0; \quad (2)$$

$$\rho\left(\frac{\partial \vec{V}}{\partial t} + (\vec{V}\nabla)\vec{V}\right) = -\nabla p + \mathrm{div}\hat{\pi}; \quad (3)$$

$$\frac{\partial U}{\partial t} + \mathrm{div}\left(\vec{V}U\right) = -p\,\mathrm{div}\vec{V} + \mathrm{div}\left(\chi\nabla T\right) + \Phi. \quad (4)$$

Here ρ, $\vec{V}$, p, and U are the density, velocity vector, pressure, and total energy of argon, respectively; $U = p/(\gamma - 1)$; $\gamma = 5/3$; χ is the thermal conductivity; and Φ is the dissipative term:

$$\Phi = \sum_{n,m} \pi_{n,m} \frac{\partial \vec{V}_n}{\partial x_m}, \quad n, m = 1\text{–}3; \quad (5)$$

$\pi_{n,m}$ are the components of the viscous strain tensor $\hat{\pi}$. The computational region (CR) represents a cylinder divided into two parts, the Pt target and ambient gas, with the axis normal to the target and coinciding with the center of the irradiation spot. The coordinate origin is located at the irradiation spot center and the coordinate z is directed towards the target. For the ambient gas region the complete set of equations (2)–(5) is solved, while for the target region the problem is reduced to solving Eq. (4) with $V = 0$. Target melting is followed via taking into account the latent heat of fusion in the U value. In the CR boundaries, the conditions of unperturbed flow (ambient gas region) and initial temperature (solid region) are kept, while at the solid-gas interface the non-slip conditions are set for the ambient gas molecules as well as the conditions of continuity for the temperature and heat flow $\chi\partial T/\partial z$. We use the splitting numerical scheme with a stabilizing correction on the shifted quasi-uniform grids.

Simulations show that the following three stages can be distinguished in the ambient gas evolution:

a) $t \sim 0$–100 ns. Sudden heating of argon adjacent to the irradiation spot results in its expansion and generation of a shock wave. The density in the heat-affected zone drops, remaining however high in a thin

layer in the immediate proximity of the irradiation spot. In this layer, an effective heat exchange takes place between the target and the ambient gas whose temperature is higher than that of the irradiated surface. In this stage, a high-temperature region is still small, of the order of 100 μm. Simulations show that the conductive heat transfer from the gas to the target is noticeable already on the ps time scale. This can explain the observed distinctions in the ablation rates in air and vacuum for sub-ps [16] and ps [17] pulses.

b) $t \sim 100$ ns – 100 μs. At a later time, the semi-spherical shock wave moves away from the irradiation spot with $V \sim 1$ km/s (Fig. 1).

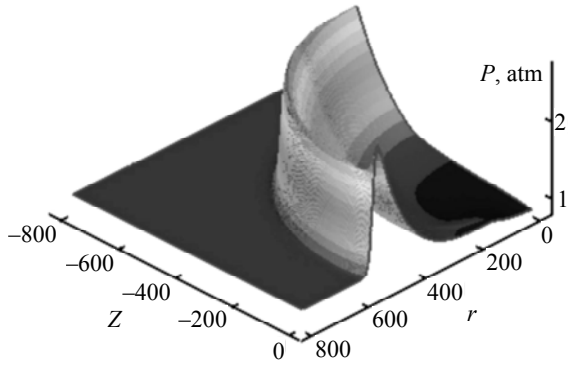

Fig. 1. The spatial pressure distributions in argon at $t = 650$ ns. The coordinates are given in μm

Behind its front, the temperature remains high, decreasing with time due to further gas expansion. At the interface between the shock wave and the target, the hot gas transfers its energy to the cold surface (Fig. 2).

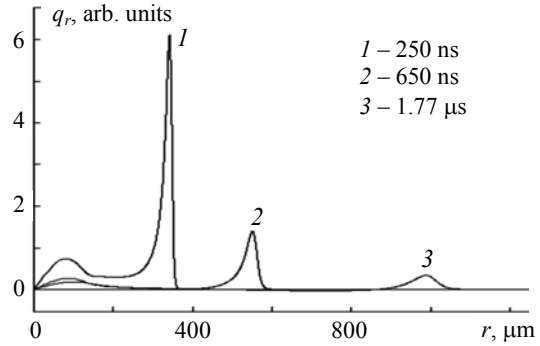

Fig. 2. The heat flux from the ambient argon to the Pt target at different time moments as a function of target radius for the conditions of Fig. 1

Such mechanism of metal target heating has been earlier proposed for μs laser pulses [11]. Namely at this stage, the main heat fraction is coupled from the ambient gas into the target causing a pronounced residual thermal effect.

c) The shock wave dissipates at $t > 100$ μs. The density and temperature level off and the pressure becomes uniform over the gas volume. However, the perturbed gas circulates near the target for a long time and provides further target heating until its temperature cools below the target elevated temperature. At ~ 0.1 s, target heating gives way to a slow cooling due to thermal losses into environment.

In view of the baffling complexity of the studied phenomenon, the above model does not take into account the ablation process and focuses only on the laser energy absorption by the ambient gas and heat exchange between the gas and the target. Also, we do not take into account the plasma radiation effect. However, we can make the following conclusions. Though the residual thermal energy effect is shown to develop mainly at a later time as compared to the ablation timescale for fs laser pulses (typically from picoseconds to a few nanoseconds) [18], plasma-assisted heating of the sample on the picosecond time scale is not negligible and can contribute to material removal. The formation of a low-density region in front of the irradiation spot indicates that the ambient gas does not counteract to material removal. However, at later stages the long-living circulation of the ambient gas near the target can result in a partial redeposition of the ablated material around the irradiation spot.

3. Breakdown kinetics

To refine the above model by considering plasma-assisted heating of the sample, we developed a modeling approach to follow the dynamics of laser-induced breakdown in the ambient. Both the irradiation conditions and the geometry of the "target – ambient gas" system are similar to those discussed in Section 2. The laser beam is assumed to enter from $-\infty$ into the volume occupied by argon (1.08 atm, 20 °C) above the Pt target. The target is located at $z = 0$ and the incoming laser light flux ε_+ evolves as follows:

$$\varepsilon_+ = \frac{F_0 s(0) \exp(-r^2/r_L^2 - (t-t_0)^2/t_L^2)}{s(-z_0)\sqrt{\pi} t_L c}. \qquad (6)$$

Here $t_L = \tau/(2\sqrt{\ln 2})$ with $\tau = 65$ fs; t_0 defines the moment of starting the simulations; c is the velocity of light; and the function $s(z) = 1 + [(z - z_t)/z_c]^2$ describes the geometry of laser beam focusing with z_t to be the distance between the target and laser focus and z_c being the length of the focusing region. When the laser beam reaches the target, the reflected flux $\varepsilon_- = R\varepsilon_+$ is formed at $z = 0$. We can write the following equations for the propagations of the incoming and reflected beams:

$$\frac{\partial(s\varepsilon_+)}{\partial t} + c\frac{\partial(s\varepsilon_+)}{\partial z} = -Q_A sk\hbar\omega \frac{\varepsilon_+}{\varepsilon_+ + \varepsilon_-}; \qquad (7)$$

$$\frac{\partial(s\varepsilon_-)}{\partial t} - c\frac{\partial(s\varepsilon_-)}{\partial z} = -Q_A sk\hbar\omega \frac{\varepsilon_-}{\varepsilon_+ + \varepsilon_-}. \qquad (8)$$

Here multi-photon ionization is expressed as $Q_A = AJ^k n_a$ where $J = J(z, t) = c(\varepsilon_+ + \varepsilon_-)$ is the local laser flux. The electron density evolution is described as

$$\frac{\partial n_e}{\partial t} = Q_A + Q_B - Q_C - Q_D, \; n_i = n_e, \; n_a = n_0 - n_e, \qquad (9)$$

where n_0 is the initial argon density; the terms Q_B, Q_C, and Q_D describe impact ionization, photo- and three-particle recombination processes respectively [19, 20]. The evolution of the electron and ion temperatures is governed by the following equations [19, 20]:

$$\frac{\left(dn_0 k_B T_i\right)}{dt} = Q_i, \quad \frac{\left(dn_e k_B T_e\right)}{dt} = Q_e, \qquad (10)$$

where Q_i and Q_e are the heat sources taking into account heat release in the ionization/recombination processes and electron-ion heat exchange [19, 20].

Figure 3 presents dynamics of the ionization process for a 65-fs laser pulse with $F_0 = 3$ J/cm^2 (we assume $z_c = 1$ mm and $z_t = 0.8$ mm).

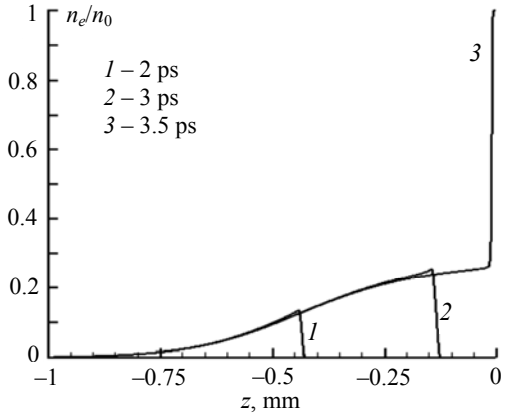

Fig. 3. The evolution of the ionization degree in argon (initial conditions are 1.08 atm, 20 °C) during propagation of the 65-fs laser pulse with fluence of 3 J/cm^2. 100% ionization occurs on reflection of the beam from the Pt target

In calculations, we use the data for Nd^{3+} laser ($A = 10^{-123}$, $k = 10.3$) [14]. With approaching the laser wave pocket to the target, the ionization wave strengthens (compare curves for 2 and 3 ps) and the ionization degree exceeds 20% already at 300 μm before the target surface. At 3.5 ps, the laser beam reflects from the target surface, and its interference results in 100% ionization in a layer of ~20 μm in front of the target. To the time of 1 ns, the argon temperature in the region of ~300 μm in front of the target exceeds 4000 K while in the interference zone the equilibrium plasma temperature is ~30000 K.

Simulations demonstrate that substantial ionization of the ambient gas takes place in front of the irradiated metallic target even at moderate laser fluences resulting in gas heating. These causes gas expansion with formation of the shock wave as was described in Section 3. As was mentioned, gas breakdown above the surface and shock wave formation can serve as a factor of modification of a laser-irradiated material.

In Figure 4 the schematic picture of plasma-breakdown modification is shown.

The target surface in contact with plasma in the shock wave is exposed to fluxes of ions, electrons, and neutrals atoms. This can results in surface modification via mechanical sputtering and chemical etching. The involved chemical processes depend on ambient gas composition and material kind and can be described in the frames adopted in plasma chemistry that is planned in our further studies.

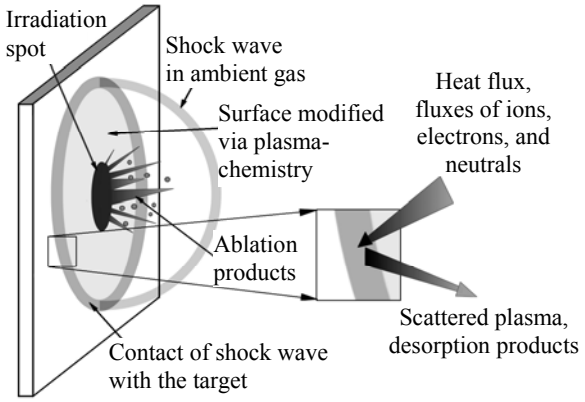

Fig. 4. Schematic representation of the processes under fs laser ablation of a target in the presence of an ambient gas. Plasma formation near the surface results in a shock wave. At a contact of the shocked plasma with the target, fluxes of the charged particles lead to surface modifications

4. Conclusion

In conclusion, the influence of ambient plasma formation on metallic target heating by fs laser pulses is studied based on 2D modeling of laser-induced target heating and the plasma dynamics. The modeling has revealed an intriguing picture of the laser-induced ambient gas motion with the formation of a strong shock wave. A model of laser-induced breakdown of an ambient gas in a prefocal region in front of the irradiated target has been proposed, which explains strong heating of ambient gas even at moderate laser fluences. We have analyzed plasma-chemical processes which can affect laser processing of surfaces in the presence of air or highly reactive media.

References

[1] D. Bäuerle, *Laser Processing and Chemistry*, 3rd ed., Springer, Verlag, 2000.
[2] B.N. Chichkov, C. Momma, and S. Nolte, et al., Appl. Phys. A **63**, 109 (1996).
[3] H.F. Winter and J.W. Coburn, Surf. Sci. Rep. **14**, 161 (1992).
[4] G. Compagnini, A.A. Scalisi, O. Puglisi, and C. Spinella, J. Mat. Res. **19**, 2795 (2004).
[5] S. Besner, A.V. Kabashin, and M. Meunier, Appl. Phys. A **88**, 269 (2007).
[6] A. Kruusing, Opt. Laser Eng. **41**, 329 (2004).
[7] A.Y. Vorobyev and C. Guo, Appl. Phys. Lett. **86**, 011916 (2005).
[8] A.Y. Vorobyev and C. Guo, Opt. Express **14**, 13113 (2006).
[9] A.N. Pirri, R.G. Root, and P.K.S. Wu, AIAA J. **16**, 1296 (1978).
[10] J.A. McKay, and R.D. Bleach, et al., J. Appl. Phys. **50**, 3231 (1979).

[11] V.P. Ageev, A.I. Barchukov, and F.V. Bunkin, et al., Sov. J. Quantum Electron. **9**, 43 (1979).
[12] S.M. Klimentov, and T.V. Kononenko, et al., Quantum Electron. **31**, 378 (2001).
[13] N.M. Bulgakova, V.P. Zhukov, A.Y. Vorobyev, and C. Guo, Appl. Phys. A, DOI 10.1007/s00339-008-4568-1.
[14] C.L.M. Ireland and C. Grey Morgan, J. Phys. D: Appl. Phys. **6**, 720 (1973).
[15] A.E. Martirosyan, and C. Altucci, et al., J. Appl. Phys. **96**, 5450 (2004).
[16] S. Preuss, A. Demchuk, and M. Stuke, Appl. Phys. A **61**, 33 (1995).
[17] E.G. Gamaly, and N.R. Madsen, et al., Phys. Rev. B **71**, 174405 (2005).
[18] K. Sokolowski-Tinten, and J. Bialkowski, et al., Appl. Surf. Sci. 127–129, 755 (1998).
[19] E.E. Lovetsky, A.N. Polyanichev, and V.S. Fetisov, Sov. J. Plasma Phys. **1**, 422 (1975).
[20] A.V. Bulgakov and N.M. Bulgakova, J. Phys. D: Appl. Phys. **28**, 1710–1718 (1995).